STRUCTURAL CONTROL AND HEALTH MONITORING
Struct. Control Health Monit. 2014; **21**:675–684
Published online 16 August 2013 in Wiley Online Library (wileyonlinelibrary.com). DOI: 10.1002/stc.1594

Reference-free delamination detection using Lamb waves

Chul Min Yeum[1], Hoon Sohn[2,*,†], Hyung Jin Lim[2] and Jeong Beom Ihn[3]

[1]*The School of Civil Engineering, Purdue University, West Lafayette, IN 47907, USA*
[2]*The Department of Civil and Environmental Engineering, Korea Advanced Institute of Science and Technology, Daejeon 305-701, South Korea*
[3]*Boeing Research & Technology, 9725 East Marginal Way South, Mail Code 42-25, Seattle, WA 98108, USA*

SUMMARY

This paper presents a new Lamb wave-based delamination detection technology that allows detection of delamination in a single wave propagation path without using prior baseline data or a predetermined decision boundary. This study shows that, if delamination exists along a wave propagation path, the first arrival antisymmetric (A_0) mode is followed by other A_0 modes reflected from the inside of the delamination. Unlike other conventional Lamb wave techniques, the proposed technique takes advantage of the first A_0 mode reflected from the inside delamination to instantly identify the existence of delamination. First, the proposed study employs a dual piezoelectric transducer (PZT), which is composed of a concentric ring and disk PZT segments, for Lamb wave excitation and a circular PZT for sensing. By activating either the circular or ring PZT segment separately, two pitch-catch Lamb wave signals are obtained from the single wave propagation path. Then, a normalized A_0 mode signal is decomposed from the measured Lamb wave signals using a previously developed mode decomposition technique, and the first A_0 mode reflected from the delamination is further extracted by using a matching pursuit algorithm. Finally, a reference-free damage classifier is built on the extracted A_0 mode reflection from the delamination. Because the proposed technique does not require baseline signals during the entire delamination detection process, robust delamination detection has been achieved even under varying temperature conditions. Copyright © 2013 John Wiley & Sons, Ltd.

Received 20 January 2013; Revised 17 May 2013; Accepted 2 July 2013

KEY WORDS: structural health monitoring; piezoelectric transducer; composite structure; delamination detection; mode decomposition; nondestructive testing

1. INTRODUCTION

Structural health monitoring (SHM) is a process to evaluate the health and performance of structures using real-time data obtained from sensors. There is an increasing interest for SHM of composite aircraft as composite materials are widely used for aircraft structures. Composite materials have many advantages over metals such as lightweight and higher strength. However, they are susceptible to damages such as delamination and disbond because of abrupt impact or accumulated fatigue loading. Such defects often occur beneath the surface of a composite aircraft, and they are hardly visible or detectable by the naked eye. Therefore, there are ongoing efforts to develop an online SHM system, which can perform automated damage diagnosis under the normal operation of an aircraft.

One of such efforts is SHM development based on Lamb wave propagation characteristics in composite structures [1–5]. In a pulse-echo mode, delamination is detected by examining waves reflected and/or scattered from the delamination [6–8]. In a pitch-catch mode, transmitted waves instead of reflected waves are analyzed for delamination detection [9–13]. Signal attenuations and time

*Correspondence to: Hoon Sohn, The Department of Civil and Environmental Engineering, Korea Advanced Institute of Science and Technology, Daejeon 305-701, South Korea.
†E-mail: hoonsohn@kaist.ac.kr

delays are commonly used features for these techniques. Furthermore, phased array transducers are used to visualize the defect location and size. An input with a proper time delay is applied to each transducer constituting the phased array, and the phased array transducers allow steering of the principal wave propagation direction and/or focusing of propagating wave energy at desired points [14,15].

These conventional techniques often operate under the following assumptions: (i) baseline signals are available from the pristine condition of the system being monitored; (ii) changes from the baseline signals can be detected and related to defects; and (iii) a decision boundary for damage diagnosis can also be established by using the available baseline signals. However, the application of these techniques to an aircraft remains challenging, because aircrafts are constantly subjected to varying temperature and external loading conditions.

To overcome this problem, damage detection techniques that are insensitive to environmental variations have been developed for composite structures [16–21]. Data normalization techniques attempt to separate the effects of environmental variations on damage diagnosis from those of structural damage by analyzing the characteristics of healthy baseline data under varying operational conditions [16,17]. Another approach is an instantaneous baseline technique, where damage is detected by comparing each signal with the other signals simultaneously obtained from a sensor network rather than by comparing each signal with its own previous baseline signal obtained from the health condition [20,21]. However, the major drawbacks of these techniques are that a large amount of baseline data needs to be recorded under varying environmental conditions or multiple instantaneous signals should be measured from other sensor paths with the same path length, specimen thickness, and material properties.

In this study, a new reference-free delamination detection technique is proposed so that delamination in a single wave path can be detected without being compared with prior baseline data or signals instantaneously obtained from multiple paths. The development of the proposed technique is based on the premise that the presence of delamination creates a unique signature that is composed of additional antisymmetric modes reflected from the inside of delamination. The existence of delamination is identified by examining the presence of the first A_0 mode reflection, followed by the first arrival (transmitted) A_0 mode. For the extraction of this A_0 mode reflection, a mode decomposition technique using a dual piezoelectric transducer (PZT) and a matching pursuit algorithm are employed [21,22,24]. Finally, reference-free delamination diagnosis is performed by using the extracted A_0 mode reflection. The effectiveness of the proposed technique is experimentally validated by using data obtained from a simple composite plate under varying temperature conditions.

This paper is organized as follows. In Section 2, the effects of delamination and temperature on Lamb wave modes are investigated. In Sections 3, the proposed reference-free delamination detection technique is formulated. The applicability of the proposed technique to delamination detection in a simple composite structure is numerically and experimentally investigated in Sections 4 and 5, respectively. The conclusion is provided in Section 6.

2. INTERACTION OF LAMB WAVES WITH DELAMINATION

In this section, the effects of delamination and temperature on Lamb wave propagation are first compared to justify the development of the proposed damage detection technique under temperature variation. Here, only a brief summary of the numerical and experimental results is presented. The pitch-catch Lamb wave signals shown in Figure 1 are experimentally obtained from the experimental setup described in Section 5. In Figures 1(a) and (b), the effect of delamination on Lamb wave signals is illustrated, whereas the temperature effect is shown in Figures 1(c) and (d). Note that the normalized A_0 mode signals in Figures 1 (b) and (d) are decomposed from the raw Lamb wave signals in Figures 1(a) and (c) using the mode decomposition technique described in Section 3.2. The findings are summarized as follows:

1. Figures 1(a) and (b) show that the A_0 mode slows down when it passes through a delamination area, whereas the speed of the S_0 mode does not change much because of delamination. Furthermore, a proportional relationship between the severity of delamination and the time delay of the A_0 mode is observed [11].

DOI: 10.1002/stc

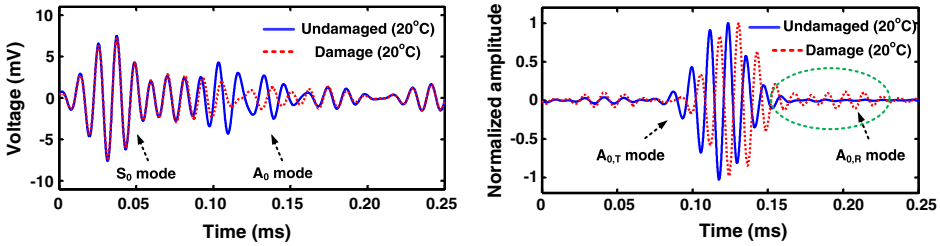

(a) Measured Lamb wave signals obtained from the undamaged and damaged conditions at 20°C

(b) Normalized A_0 mode signals obtained from the undamaged and damaged conditions at 20°C

(c) Measured Lamb wave signals obtained from the undamaged conditions at 20°C and 50°C

(d) Normalized A_0 mode signals obtained from the undamaged conditions at 20°C and 50°C

Figure 1. Comparison of the normalized A_0 mode signals obtained from undamaged and damaged conditions and from different temperatures (experiment data obtained from the experiment described in Section 5): the normalized A_0 mode signals in Figure 1(b) and (d) are decomposed from raw Lamb wave signals in Figure 1(a) and (c), respectively. In Figure 1 (b), the first A_0 mode reflected from the inside delamination (denoted as the $A_{0,R}$ mode) is clearly observed arriving after the transmitted A_0 mode (denoted as the $A_{0,T}$ mode).

2. As delamination increases, the amplitudes of the A_0 modes are slightly amplified initially and followed by attenuation with a further increase of delamination. A similar initial amplification of the A_0 mode is also reported by the others [11].
3. A numerical simulation also reveals that the A_0 modes are more significantly delayed and attenuated by delamination than the S_0 modes. This is because delamination primarily decreases interlaminar shear strength, and the A_0 modes are dominantly affected by the shear modulus of the specimen.
4. Mode conversion occurs because of delamination, but the converted modes rapidly attenuate, making it difficult to reliably measure the converted modes. The numerical simulation shows that the amplitude of the converted modes because of delamination is typically less than 1% of the amplitudes of the A_0 and S_0 modes.
5. The waveforms of the A_0 and S_0 modes are hardly distorted by delamination because the frequency content of the propagating waves is little affected by delamination.
6. Figure 1(b) shows that when the A_0 mode interacts with delamination, some portion of the A_0 modes passes through the delamination, and the other is transmitted after bouncing back and forth once or multiple times from the entrance and exit boundaries of the delamination. Hereafter, the A_0 mode passing directly through the delamination and the first reflected A_0 mode from the delamination are denoted as $A_{0,T}$ and $A_{0,R}$ modes, respectively. Note that only the $A_{0,R}$ mode is used for the proposed damage diagnosis technique, and the influence of subsequent reflections is ignored.

Next, the effect of temperature is investigated in Figures 1(c) and (d). Similar to the effect of delamination, the amplitude and arrival time of the A_0 modes are affected by temperature variation. More specifically, as temperature increases, the A_0 mode amplitude decreases, and the arrival time of the A_0 modes is delayed. However, the S_0 mode characteristics are rarely affected by temperature. Additional A_0 modes because of mode conversion or internal reflections are not observed under temperature variation.

DOI: 10.1002/stc

These observations reveal the challenge of applying the conventional damage detection techniques to an in-flight aircraft. Because of the similarity of delamination and temperature effects, delamination detection under varying temperature conditions becomes challenging. To address this issue, the proposed technique takes advantage of the $A_{0,R}$ mode as a unique feature that can separate delamination from temperature variation. In the next section, the proposed delamination detection technique built on this unique damage feature is introduced.

3. REFERENCE-FREE DELAMINATION DETECTION TECHNIQUE

Here, the overall procedure of the proposed delamination detection technique is described. First, two pitch-catch Lamb wave signals are obtained by separately exciting two parts of the dual PZT and measuring the corresponding responses by using a circular PZT. Second, the normalized A_0 mode signal is decomposed by using the previously developed mode decomposition technique [19,23]. Third, the $A_{0,R}$ mode is extracted from the normalized A_0 mode signal using the matching pursuit algorithm described in Section 3.3. Once the $A_{0,R}$ mode is extracted, the proposed damage detection technique identifies the existence of delamination on the basis of the $A_{0,R}$ mode.

3.1. Sensor design and layout

Figure 2(a) shows the schematic drawing of the dual PZT used in this study. The dual PZT is composed of concentric inner circular and outer ring PZTs, which can be selectively activated for actuation [19,23]. Signal Ab denotes a response measured by the circular sensing PZT B (denoted as PZT B), when the outer ring of the dual PZT A (denoted as PZT A) is actuated. Similarly, signal ab is the response of PZT B corresponding to the excitation of the inner disk of PZT A. The darker (red) areas in Figure 2(b) show the PZT parts activated for either Lamb wave excitation or sensing.

3.2. Decomposition of the normalized A_0 mode signal

Because the A_0 modes are more sensitive to delamination than the S_0 modes are, the first step of the proposed delamination detection technique is to decompose only the A_0 modes from the measured Lamb signals. Because S_0 modes travel faster than A_0 modes, the S_0 modes reflected from structural boundaries can frequently overlap with the A_0 modes, making this mode decomposition process necessary. This decomposition is particularly essential for composite structures because the difference between S_0 and A_0 mode group velocities is larger in composite structures than in metallic structures.

The theoretical detail of the mode decomposition techniques can be found in [22], and only a brief summary is provided here for the completeness of the paper. Figure 3 shows that the mode decomposition technique isolates the A_0 modes by properly scaling two signals obtained from the same path but with two

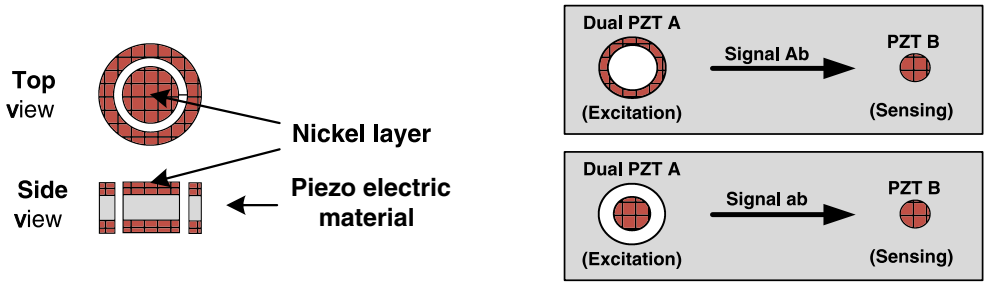

(a) A schematic drawing of the dual PZT (b) Notations of signals

Figure 2. A schematic drawing of the dual PZT and examples of signals obtained by a pair of the dual PZT and the circular PZT: signal Ab denotes a response measured by the circular sensing PZT B (denoted as PZT B), when the outer ring of the exciting dual PZT A (denoted as PZT A) is used for excitation. Similarly, signal ab is the response of PZT B corresponding to the excitation of the inner circular part of PZT A. The darker (red) areas of PZTs A and B represent the PZT component activated either for excitation or sensing.

DOI: 10.1002/stc

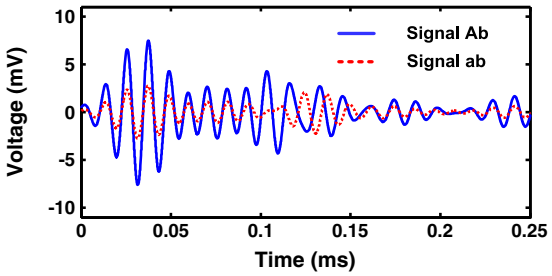

(a) Signals Ab and ab

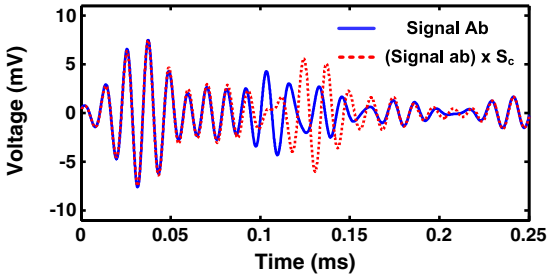

(b) Subtraction of Signal Ab from scaled Signal ab

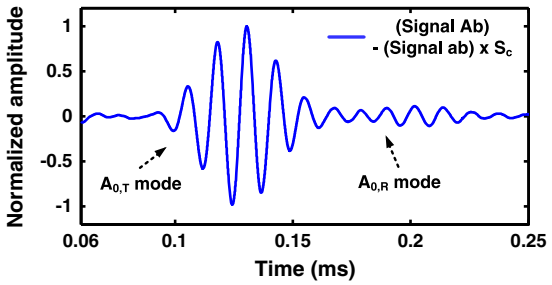

(c) Decomposition of only the A_0 mode

Figure 3. Illustration of the decomposition of the normalized A_0 mode signal using the mode decomposition technique: signals Ab and ab are measured from a path with delamination described in Section 5. S_c is the amplitude ratio of the S_0 mode of signal Ab to that of signal ab.

different excitation PZT sizes. The Lamb wave excitation at the same position but with different PZT sizes is made possible using the prescribed dual PZT. The procedure can be summarized as follows:

1. In a pitch-catch mode, signals Ab and ab are measured at PZT B when the outer ring and inner disk parts of PZT A are actuated separately as shown in Figure 3(a).
2. In Figure 3(b), signal ab is scaled by S_c so that the S_0 modes in signals Ab and ab have the same amplitude. S_c is the amplitude ratio of the S_0 mode of signal Ab to that of signal ab.
3. By subtracting scaled signal ab from signal Ab, the S_0 mode is removed and only the normalized A_0 mode signal remains as shown in Figure 3(c).

Once the normalized A_0 mode signal is decomposed, it is proceeded to the next step to extract the $A_{0,R}$ mode, which may exist.

3.3. Mode extraction using a matching pursuit algorithm

A matching pursuit algorithm is employed in this study to extract the $A_{0,R}$ mode from the decomposed normalized A_0 mode signal [21,24]. The matching pursuit algorithm is a signal processing technique that iteratively decomposes a target time signal into a linear combination of basic functions. At the first iteration, the parameters of the first basis function, such as arrival time, scale, and amplitude, are optimized so that the target signal can be best projected on to the first basis function. Next, the residual

DOI: 10.1002/stc

signal, which is the remaining component of the target signal after projection onto the first basis function, is now projected onto the second basis function. These steps are repeated until all wave components of interest are identified and extracted. In this study, this technique allows two dominant wave components, the $A_{0,T}$ and $A_{0,R}$ modes, to be extracted from the previously decomposed normalized A_0 mode signal. A more detailed description on the matching pursuit algorithm can be found in [24,25].

In Figure 4, the matching pursuit algorithm is applied to the decomposed normalized A_0 mode signal (denoted as original) in Figure 3(c). The $A_{0,T}$ and $A_{0,R}$ modes are well separated from the original. In practice, an additional layer of decision making is, however, necessary to determine if this appearance of the $A_{0,R}$ mode is a true indication of delamination beyond a background noise level. To tackle this issue, a damage classifier is developed in Section 3.4.

3.4. Damage classification

When the previously decomposed normalized A_0 mode signal is denoted as M_0, the first and second wave packets are extracted from M_0 and denoted as M_1 and M_2, respectively. Here, M_1 is definitely the $A_{0,T}$ mode, but it is not clear whether M_2 is an additional wave packet produced by delamination or simply a noise component. If M_2 represented the simple noise component, it could be assumed that an error signal defined as $e = M_0 - M_1 - M_2$ has a Gaussian distribution with a zero mean and standard deviation of σ_e. Once σ_e is estimated from the error signal, the upper ($3\sigma_e$) and lower ($-3\sigma_e$) limits corresponding to a 99.7% confidence interval are computed. If M_2 is indeed produced by delamination, which is the $A_{0,R}$ mode, its amplitude would increase and exceed either the upper or lower limit, indicating the presence of the delamination [19]. Note that the decision boundaries in this approach are instantaneously computed only from the current data set, and they continuously change because of ambient variations such as temperature.

4. NUMERICAL SIMULATION

4.1. Description of the simulation setup

In this section, numerical simulation is performed to investigate the interaction of Lamb waves with delamination and A_0 mode decomposition and extraction capabilities. A commercially available finite element analysis program (MSC/NASTRAN, MSC Software Corporation, 2 MacArthur Place, Santa Ana, California) and a pre-processor and post-processor (PATRAN) are used for the simulation. For the numerical simulation, a 3-D plate structure of $520 \times 460 \times 3$ mm is simulated as shown in Figure 5. The PZT is assumed to be perfectly bonded to the structure, and no PZT damping is considered. The input force exerted by the excitation dual PZT is modeled as 'pin forces' applied along equally spaced multiple points among the circumferential boundary of the PZT [22]. The corresponding output response is computed by integrating the strain over the sensing PZT that is meshed on the structure. One dual PZT and one circular PZT are modeled on the top surface of the plate.

Delamination can be modeled by reducing the shear modulus in a delaminated area because the delamination, such as transverse crack, causes significant reduction in the shear modulus of an original structure [26]. In this study, the shear modulus of the delamination area is reduced to 70% of the original shear modulus, and its size is $10 \times 30 \times 3$ mm as shown in Figure 5.

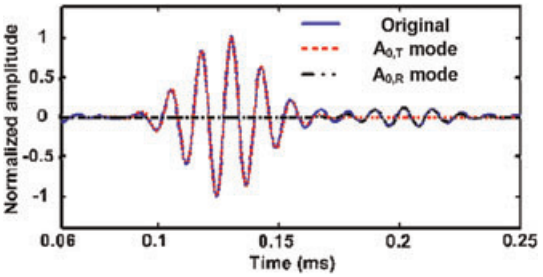

Figure 4. Illustration of the A_0 mode extraction using the matching pursuit algorithm.

DOI: 10.1002/stc

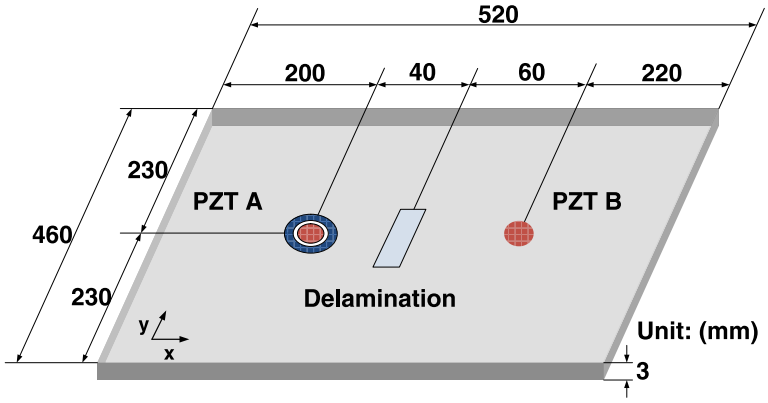

Figure 5. The dimension and configuration of the plate structure used in the numerical simulation.

The driving frequency of a tone burst input waveform is selected to be 100 kHz so that only the S_0 and A_0 modes are generated and sensed. The maximum mesh size is $1 \times 1 \times 1$ mm, and the sampling rate of 5 ms/s is chosen to be sufficiently high to capture the smallest traveling wavelength. Rayleigh damping coefficients for the plate model were set to 10^{-4} for a mass damping coefficient and 0 for a stiffness damping coefficient, respectively.

4.2. Simulation results

Figure 6(a) compares raw signals measured from undamaged and damage conditions. The comparison shows that the A_0 modes slow down and attenuate when it passes through a delamination area, whereas the speed and amplitude of the S_0 modes do not change much at delamination. Because the S_0 modes reflected from structural boundaries has a larger amplitude than the amplitude of the $A_{0,R}$ mode and the reflected S_0 modes overlap with the $A_{0,R}$ mode, the existence of the $A_{0,R}$ mode cannot be clearly identified from the raw signal corresponding to the damage case in Figure 6(a). On the other hand, the existence of the $A_{0,R}$ mode becomes apparent in Figure 6(b) when the A_0 mode signal is decomposed from the raw signal using the mode decomposition technique described in Section 4.

Next, the effectiveness of the matching pursuit algorithm for the extraction of the $A_{0,T}$ and $A_{0,R}$ modes is successfully demonstrated in Figure 7. Here, the first and second reflections indicate the A_0 modes measured at the sensing PZT after bouncing back and forth between the entrance and exit boundaries of the delamination once and twice. As mentioned previously, the proposed damage detection technique focuses on the identification of the $A_{0,R}$ mode, because the second reflection is hardly observed in real experiments.

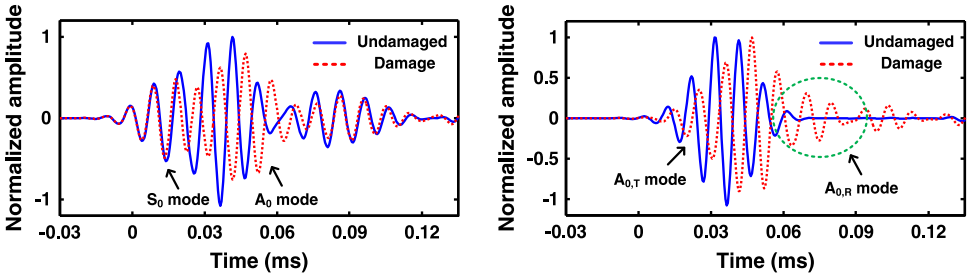

(a) Raw signals obtained from undamaged and damaged conditions

(b) Normalized A_0 mode signals obtained from undamaged and damaged raw signals

Figure 6. Comparison of the Lamb wave signals obtained from undamaged and damaged conditions (numerical simulation): The $A_{0,R}$ mode and the subsequent reflection are clearly observed if delamination exists.

DOI: 10.1002/stc

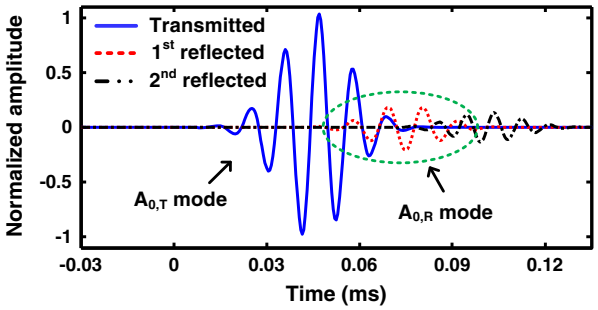

Figure 7. The A_0 modes extracted from a damaged condition: The '1st reflected' and '2nd reflected' are the A_0 modes measured at the sensing PZT after bouncing back and forth between the entrance and exit boundaries of the delamination once and twice, respectively.

5. DELAMINATION DETECTION IN A COMPOSITE SPECIMEN

5.1. Description of the experimental setup

To validate the proposed delamination detection technique, a multilayer carbon fiber composite plate shown in Figure 8(a) is tested. The proprietary material properties and prepreg lay-up information of the specimen are unknown to the authors. The dimensions of the specimen are $1512 \times 762 \times 5$ mm, and a dual PZT and a circular PZT, denoted as PZT A and PZT B, are installed on the inside surface of the specimen using a high strength adhesive. The spacing between PZT A and PZT B are 120 mm. PZT A is composed of inner circular and outer ring PZTs. The radius of the circular PZT and the inner and outer radii of the exterior ring PZTs are 2, 3, and 4 mm, respectively. The radius of PZT B is 5 mm, and the thickness of both PZTs is 0.5 mm. A conventional drop weight impact tester with a 10-mm-radius steel ball tip is used to introduce low velocity impact damage. Two consecutive impacts are applied to a single point 50 mm away from PZT A, exerting 24.5 J each time.

The data acquisition system and temperature chamber used in this study are shown in Figure 8(b). The data acquisition system consists of an arbitrary waveform generator, a high-speed signal digitizer, a low-noise preamplifier, a high-power amplifier, and a multiplexer. A 7-cycle tone burst signal with a 10 peak-to-peak voltage is generated by using the 14-bit arbitrary waveform generator. The response signals are measured 20 times and averaged in the time domain to improve the signal-to-noise ratio. An excitation frequency of 80 kHz is selected so that only A_0 and S_0 modes exist, and the A_0 mode is more dominant than the S_0 mode. Damage diagnosis is performed under changing temperature conditions of 20 and 50 °C using a temperature chamber.

5.2. Experimental results

Figures 1(a) and (c) show raw Lamb wave signals measured from the intact and damage conditions of the test articles at 20 and 50 °C, respectively. The corresponding normalized A_0 mode signals decomposed from the raw signals are shown in Figures 1(b) and (d). The mode decomposition process is outlined in Figure 3. Next, the decomposed normalized A_0 mode signal is broken apart into the first

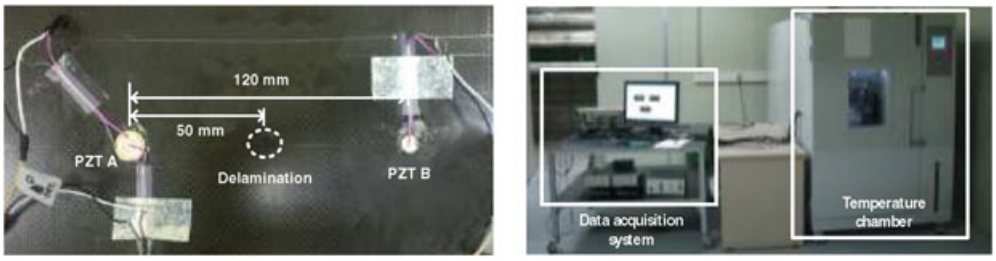

(a) A composite plate with PZTs (b) Data acquisition system and temperature

Figure 8. Testing configuration for detecting delamination on a composite plate.

DOI: 10.1002/stc

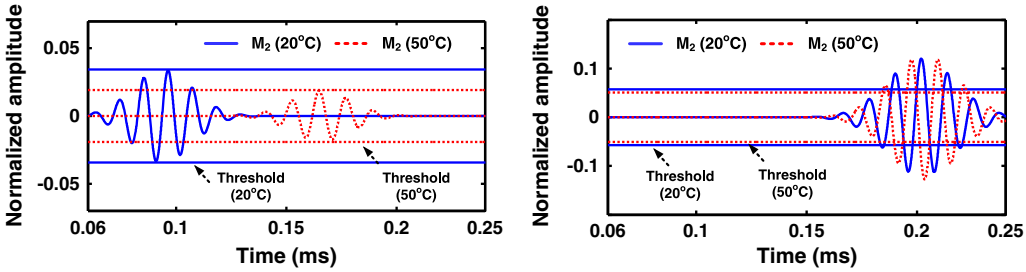

(a) Without damage (b) With damage

Figure 9. Autonomous reference-free damage classification under changing temperature conditions: if delamination exists, the amplitude of each second wave packet (M_2) in both temperature conditions exceeds the corresponding threshold values. Note that the decision boundary (threshold values) in each M_2 is instantaneously computed only from the current measurement signal, and the threshold values continuously change because of ambient variations such as temperature.

and second wave packets using the matching pursuit algorithm. Figure 4 shows the $A_{0,T}$ and $A_{0,R}$ modes extracted for the delamination condition using the matching pursuit algorithm.

Once extracting the first and second wave packets, the proposed damage classification is performed. The second wave packet (M_2) and the corresponding threshold value are used for damage classification, described in Section 3.4. In the absence of delamination, the amplitude of M_2 do not exceed the corresponding threshold values, and no false alarms are produced in both 20 and 50 °C conditions (Figure 9(a)). However, when delamination is introduced, the amplitude of M_2, which is the $A_{0,R}$ mode, exceeds the corresponding threshold values, successfully identifying delamination (Figure 9(b)).

6. CONCLUSION

In this study, a new reference-free delamination technique is developed so that delamination in a multilayer composite plate can be detected by identifying the presence of the A_0 mode reflection produced by delamination. Numerical simulation and experimental testing are conducted to investigate the interaction between the A_0 mode and delamination. The effectiveness of the proposed delamination detection technique is demonstrated by using the experimental test data obtained from a multilayer composite plate. An impact induced delamination is successfully identified, whereas no false-positive alarms are produced for the undamaged conditions even under temperature variation.

ACKNOWLEDGEMENTS

This work is supported by the Boeing Company, the Radiation Technology Program (M20703000015-07 N0300-01510), and the Nuclear Research & Development Program (2009-0083489) of National Research Foundation of Korea (NRF) funded by Ministry of Education, Science & Technology (MEST).

REFERENCES

1. Raghavan A, Cesnik CES. Review of guided-wave structural health monitoring. *Shock and Vibration Digestion* 2007; **39**:91–114.
2. Kessler SS, Spearing SM, Soutis C. Damage detection in composite materials using Lamb wave methods. *Smart Materials and Structures* 2002; **11**:269–278.
3. Giurgiutiu V, Cuc A. Embedded non-destructive evaluation for structural health monitoring, damage detection, and failure prediction. *Shock and Vibration Digestion* 2005; **37**:83–105.
4. Su Z, Ye L, Lu Y. Guided Lamb waves for identification of damage in composite structures: a review. *Journal of Sound and Vibration* 2006; **295**:753–780.
5. Lu Y, Michaels JE. A methodology for structural health monitoring with diffuse ultrasonic waves in the presence of temperature variations. *Ultrasonics* 2005; **43**:717–731.
6. Ip KH, Mai YW. Delamination detection in smart composite beams using Lamb waves. *Smart Materials and Structures* 2004; **13**:544–551.
7. Yang M, Qiao P. Modeling and experimental detection of damage in various materials using the pulse-echo method and piezoelectric sensors/actuators. *Smart Materials and Structures* 2005; **14**:1083–1100.
8. Lestari W, Qiao P. Application of wave propagation analysis for damage identification in composite laminated beams. *Journal of Composite Materials* 2005; **39**:1967–1984.

DOI: 10.1002/stc

9. Toyama N, Noda J, Okabe T. Quantitative damage detection in cross-ply laminates using Lamb wave method. *Composites Science and Technology* 2003; **63**:1473–1479.
10. Guo N, Cawley P. The interaction of Lamb waves with delaminations in composite laminates. *The Journal of the Acoustical Society of America* 1993; **94**:2240–2246.
11. Petculescu G, Krishnaswamy S, Achenbach JD. Group delay measurements using modally selective Lamb wave transducers for detection and sizing of delaminations in composites. *Smart Materials and Structures* 2007; **17**:015007.
12. Ihn JB, Chang FK. Pitch-catch active sensing methods in structural health monitoring for aircraft structures. *Structural Health Monitoring* 2008; **7**:5–19.
13. Wang D, Ye L, Lu Y, Su Z. Probability of the presence of damage estimated from an active sensor network in a composite panel of multiple stiffeners. *Composites Science and Technology* 2009; **69**:2054–2063.
14. Yu L, Giurgiutiu V. In situ 2-D piezoelectric wafer active sensors arrays for guided wave damage detection. *Ultrasonics* 2008; **48**:117–134.
15. Yan F, Rose JL. Guided wave phased array beam steering in composite plates, health monitoring of structural and biological systems. *Proceedings of SPIE* 2007; **6532**:65320G.
16. Lim HJ, Kim MK, Sohn H, Park CY. Impedance based damage detection under varying temperature and loading conditions. *NDT & E International* 2011; **44**:740–775.
17. Oh CK, Sohn H. Statistical novelty detection within the Yeongjong suspension bridge under environmental and operational variations. *Structural Health Monitoring* 2009; **18**:125022.
18. Ruzzene M, Xu B, Lee SJ, Michaels TE, Michaels JE. Damage visualization via beamforming of frequency-wavenumber filtered wavefield data. *Proceedings of SPIE* 2010; **7650**:76500L.
19. Sohn H, Kim SB. Development of dual PZT transducers for reference-free crack detection in thin plate structures. *IEEE Transactions on Ultrasonics, Ferroelectrics, and Frequency Control* 2010; **57**:229–240.
20. Anton SR, Inman DJ. Reference-free damage detection using instantaneous baseline measurements. *The American Institute of Aeronautics and Astronautics* 2009; **47**:1952–1964.
21. Yeum CM, Sohn H, Ihn JB. Delamination detection in a composite plate using a dual piezoelectric transducer network. *Proceedings of SPIE* 2011; **7984**:798406.
22. Yeum CM, Sohn H, Ihn JB. Lamb wave mode decomposition using concentric ring and circular piezoelectric transducers. *Wave Motion* 2010; **48**:358–370.
23. http://www.metisdesign.com (accessed 15 March 2012).
24. Hong JC, Sun KH, Kim YY. The matching pursuit approach based on the modulated Gaussian pulse for efficient guided wave damage detection. *Smart Materials and Structures* 2005; **14**:548–560.
25. Mallat SG, Zhang Z. Matching pursuits with time-frequency dictionaries. *IEEE Transactions on Signal Processing* 1993; **41**(12):3397–3415.
26. Sun CT, Potti SV. A simple model to predict residual velocities of thick composite laminates subjected to high velocity impact. *International Journal of Impact Engineering* 1996; **18**(3):339–353.

DOI: 10.1002/stc